



Exploiting bacterial peptide display technology to engineer biomaterials for neural stem cell culture

Lauren E. Little ^a, Karen Y. Dane ^b, Patrick S. Daugherty ^b, Kevin E. Healy ^{c,d}, David V. Schaffer ^{a,c,e,*}

^a Department of Chemical Engineering, University of California at Berkeley, Berkeley, CA 94720, United States

^b Department of Chemical Engineering, University of California at Santa Barbara, Santa Barbara, CA 93106, United States

^c Department of Bioengineering, University of California at Berkeley, Berkeley, CA 94720, United States

^d Department of Material Science and Engineering, University of California at Berkeley, Berkeley, CA 94720, United States

^e The Helen Wills Neuroscience Institute, University of California at Berkeley, Berkeley, CA 94720, United States

ARTICLE INFO

Article history:

Received 28 September 2010

Accepted 15 October 2010

Available online 3 December 2010

Keywords:

Biomimetic material

ECM

Peptide

Stem cell

ABSTRACT

Stem cells are often cultured on substrates that present extracellular matrix (ECM) proteins; however, the heterogeneous and poorly defined nature of ECM proteins presents challenges both for basic biological investigation of cell-matrix investigations and translational applications of stem cells. Therefore, fully synthetic, defined materials conjugated with bioactive ligands, such as adhesive peptides, are preferable for stem cell biology and engineering. However, identifying novel ligands that engage cellular receptors can be challenging, and we have thus developed a high throughput approach to identify new adhesive ligands. We selected an unbiased bacterial peptide display library for the ability to bind adult neural stem cells (NSCs), and 44 bacterial clones expressing peptides were identified and found to bind to NSCs with high avidity. Of these clones, four contained RGD motifs commonly found in integrin binding domains, and three exhibited homology to ECM proteins. Three peptide clones were chosen for further analysis, and their synthetic analogs were adsorbed on tissue culture polystyrene (TCPS) or grafted onto an interpenetrating polymer network (IPN) for cell culture. These three peptides were found to support neural stem cell self-renewal in defined medium as well as multi-lineage differentiation. Therefore, bacterial peptide display offers unique advantages to isolate bioactive peptides from large, unbiased libraries for applications in biomaterials engineering.

© 2010 Elsevier Ltd. All rights reserved.

1. Introduction

Many cell types, including stem cells, require interactions with extracellular matrix (ECM) molecules to support and regulate their survival and proliferation [1,2]. In addition to serving as important structural elements in formations such as basement membrane, the ECM exhibits a number of bioactivities via engaging with cellular adhesion receptors such as integrins, thereby activating a number of downstream signaling pathways including crosstalk with growth factor dependent pathways [3–6]. As a result, ECM molecules regulate a number of downstream cell behaviors, including adhesion, survival, proliferation, migration, and differentiation [7]. These many active roles of ECM molecules explain why many surfaces do not support the growth of stem cells [8,9].

Although animal- and human-derived ECM molecules are often necessary for current stem cell culture systems, their use is highly problematic for numerous reasons. Natural ECM molecules are very large (e.g. ~500,000 MW fibronectin and ~850,000 MW laminin), are extremely complex (with numerous isoforms, splice variants, and glycoforms), and have numerous signaling motifs that are not yet fully understood [10]. In addition, there is considerable lot-to-lot variability in animal- and human-derived ECM because of the many isoforms present and difficulty in purifying such proteins to homogeneity [11,12], and such protein preparations run the risk of being contaminated with pathogens and immunogens [13]. The development of stem cell culture systems that are robust, reproducible, and scaleable can benefit both scientific studies and clinical therapies.

One promising approach is to design and develop synthetic stem cell culture platforms that mimic the physical and biochemical properties of the natural ECM. For example, materials can be functionalized with short (9–15mer) synthetic peptide ligands designed to engage with cell-surface receptors and thereby functionally replace ECM proteins typically used in stem cell culture [9,12,14–17]. In particular, it is important to develop surfaces that

* Corresponding author. Department of Chemical Engineering, 274 Stanley Hall, University of California at Berkeley, Berkeley, CA 94720-3220, United States. Tel.: +510 643 5963; fax: +510 642 4778.

E-mail address: schaffer@berkeley.edu (D.V. Schaffer).

can engage with integrins—heterodimeric transmembrane receptors that bind ECM molecules, anchor cells to the matrix, and act as bidirectional transducers to transmit both mechanical and chemical stimuli into the cell [18–20]. Most ligands for integrins that have been exploited in biomaterials research have employed the canonical Arg-Gly-Asp (RGD) sequence that binds a subset of these adhesion receptors [21–24]. The flanking residues to the RGD sequence can affect specificity to the RGD-binding integrins such as the $\alpha_v\beta_3$ integrin [22,24]. However, identifying new ligands that bind these and other receptors could aid in engineering biomaterials and production of cell-based therapies for the clinic, as well as in gaining a better understanding of signaling mechanisms that regulate cell function [23,25–28].

However, while various cell-binding domains—such as RGD and IKVAV motifs—[29,30] have been identified in many ECM proteins, many peptides mimicking those domains are not as active as the full ECM proteins, as evidenced by the fact that few of them support the culture of cells to the same extent of the native protein [12,29–36]. In addition, many of the important signaling domains in ECM proteins may not be known, and for example only recently has the α_v integrin binding domain in fibronectin been identified [37]. Finally, in general there is no guarantee that the optimal peptide ligand for a given receptor exactly matches a portion of the “linear” sequence of its natural ECM ligand, because the three-dimensional structure of proteins that typically contain more than one chain (e.g., laminin, collagen). Therefore, there is a need to develop a robust method to identify new candidate peptides that can be used to modify or create biomaterials to replace ECM proteins.

Due to the vast number of possible peptide sequences, even for a very short polypeptide, rationally designing such a ligand is very challenging; however, library-based screening and selection methods have potential to address this problem. With library strategies such as bacterial display, many peptides with random sequences can be tested simultaneously and thus can facilitate the discovery of peptides even with little prior mechanistic knowledge of the motifs required for receptor engagement [38,39]. While phage display libraries have been used in a number of prior studies, these have focused primarily on finding cell adhesion receptors antagonists, including for integrins, rather than identifying peptides agonists for these receptors [40–44]. In addition, newer library systems using bacteria as a display platform offer numerous advantages. For example, they are easier to generate

since the libraries involve straightforward plasmid manipulations, do not require bacteriophage production or purification, do not involve viral infection steps for amplification during the selection process, and can readily be analyzed after selection by simple plasmid isolation and sequencing [38,39,45–47]. In addition, the levels of surface-displayed peptide can in principle be varied to modulate selection stringency, and fluorescent protein expressing bacteria can be used to aid library selection and analysis [48–50].

In this study, we have used a bacterial display library to identify new peptides that bind adult hippocampal neural stem cells (NSCs). Several of these peptides were examined for their ability to support neural stem cells in two different contexts: adsorbed on tissue culture polystyrene (TCPS) or grafted to an interpenetrating polymer network surface. On both surfaces, neural stem cells retained their ability to self-renew or differentiate into multiple lineages, depending on the soluble factors given to the cells.

2. Materials and methods

2.1. Cell culture

Neural stem cells isolated from the hippocampal region of the adult rat brain were cultured on polyornithine/laminin adsorbed to tissue culture polystyrene plates as described elsewhere [1,51]. These cells were grown in DMEM/F12 media (Invitrogen) supplemented with N-2 (Invitrogen) and 20 ng/mL recombinant human fibroblast growth factor 2 (FGF-2) (Peprotech).

2.2. Bacterial Peptide display libraries

The bacterial display libraries were expressed in MC1061 *Escherichia coli* carrying a pBAD33 plasmid encoding alajGFP and the CPX membrane protein—a circularly permuted form of the common bacterial protein OmpX to locate the N- and C-terminus on its extracellular face [52]—with random peptides of the forms X₁₅ (15mer) and X₂CX₇CX₂ (7C) displayed from the N-terminus [50]. Three libraries were used: one containing only 15mer clones (15), one containing only 7C clones (7C), and a third with initially equal parts of 15mer and 7C clones (combined). alajGFP is a bright fluorescent protein engineered for high expression in *E. coli* [48], and both genes were expressed under the control of an arabinose-inducible promoter.

2.3. Bacterial peptide display selections

The central approach of this study (Fig. 1) integrates bacterial peptide display library selection with biomaterials engineering. Peptide selections were performed in three rounds based on the method of Dane et al. [50]. In each round, a frozen stock of the bacterial library was grown overnight in Luria Broth (LB) supplemented with 34 µg/mL chloramphenicol (Sigma) and 0.2% D-glucose (Sigma). The library was then

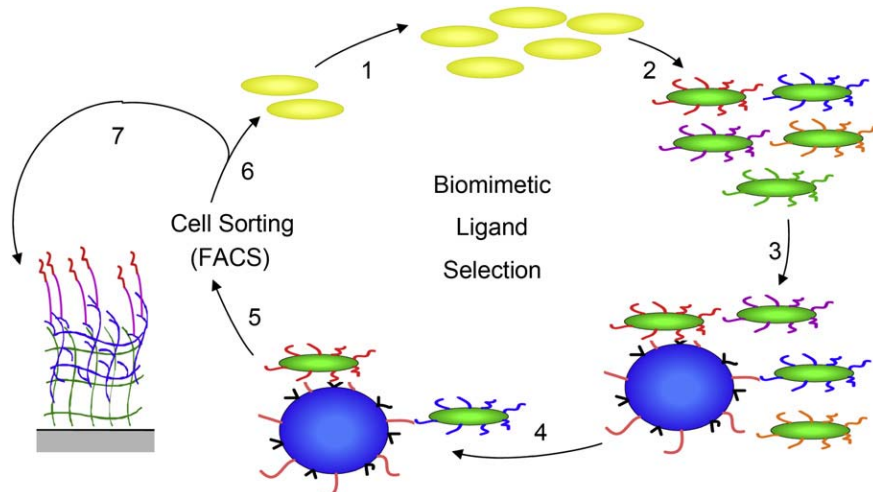


Fig. 1. Schematic of biomimetic ligand selection and incorporation into biomaterials. (1) Bacterial libraries are expanded. (2) Co-expression of green fluorescent protein and bacterial outer membrane protein CPX with the displayed peptide are induced with arabinose. (3) Stem cells are added to bacterial libraries in a co-incubation step in which the bacteria can bind to the stem cell surface. (4) Non-adherent bacteria are washed away with low speed co-centrifugation. (5) For third round selections or analysis of bacterial populations, samples of the stem cells are sorted or analyzed on a fluorescence activated cell sorter or flow cytometer. (6) Bacteria populations are frozen or plated for further selection or analysis. (7) Peptides from clones are sequenced. Synthetic versions of these peptides are then conjugated on biomaterials.

sub-cultured 1:50 with LB and 34 µg/mL chloramphenicol. After 2 h, it was induced at 30 °C with 0.02% L-arabinose (Sigma) to initiate expression of *alajGFP* [48] and CPX. Neural stem cells were removed from their plates with 2 mM Na₂EDTA (Fisher) in phosphate-buffered saline (PBS) and then co-incubated with the bacteria in a shaker for 1 h in DMEM/F12 media.

For the first round, 100-fold more bacterial cells than NSCs were used, and 50-fold more were used for the latter two rounds. Washing steps were performed by centrifuging the samples at 3500 rpm for 4 min for the first round and 1600 rpm for 30 s for the subsequent rounds. The resulting pellet was then grown overnight in LB supplemented with 34 µg/mL chloramphenicol and 0.2% D-glucose. For the third round selections, FACS was performed on the samples after the washing using a Beckman Coulter Elite Sorter instrument in the Berkeley Flow Cytometry Lab. Clonal and library analysis was performed with flow cytometry after the bacteria population was panned against NSCs similar to third round selections. All libraries were analyzed by expanding 10⁸ clones of each library. Representative flow cytometry data were analyzed with Flowjo software. The resulting populations from these selections were then either plated or frozen for further selection or later analysis. After all selections, some of the resulting bacterial clones with high avidity to the mammalian cell surface of interest were sequenced.

2.4. Synthetic peptides

Synthetic peptides for all studies were purchased from American Peptide Company, Inc. Linear peptides had an additional cysteine residue on the N-terminus

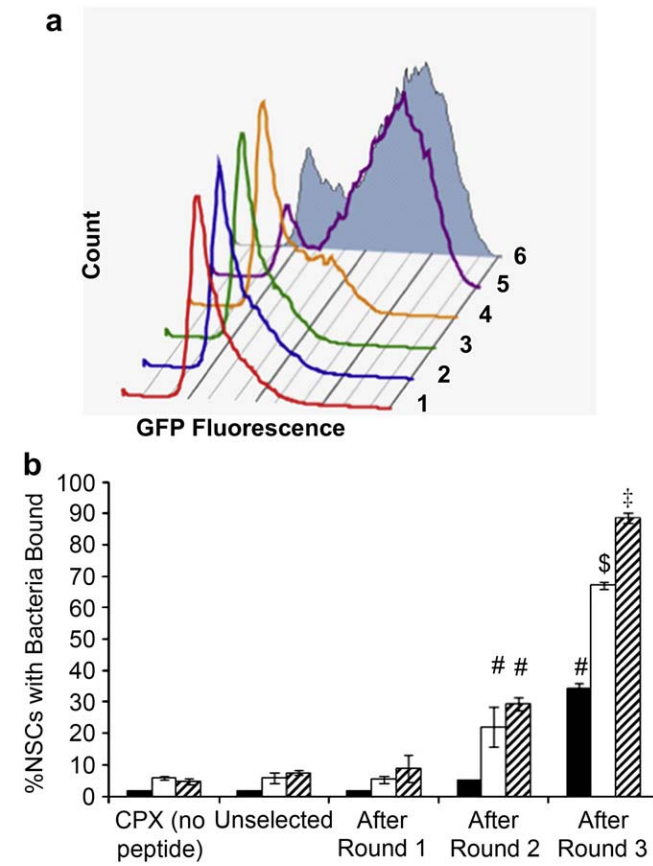


Fig. 2. Binding capacity of peptide display library populations with neural stem cells. (a) Example histograms of library and clonal populations of the bacterial peptide display libraries binding to neural stem cells: (1) CPX (no peptide), (2) unselected 7C library, (3) 7C library after Round 1, (4) 7C library after Round 2, (5) 7C library after Round 3, and (6) high affinity clone 15-2. (b) Quantification of library populations. Three libraries were tested: (■) 15mer library composed of peptides with the sequence X₁₅, (▨) 7C library composed of peptides with the sequence X₂CX₇CX₂, and (□) a combined library containing both types of peptide clones. All unselected and post round 1 library populations showed similar binding as bacteria expressing CPX, the outer membrane display protein, but no peptide. After rounds 2 and 3, there were significantly more bacteria binding to the neural stem cells, with the 7C library having the highest amount of binding. The 15mer and in particular the combined libraries exhibited the highest binding. Data represent mean ± standard deviation. Library populations not in the same group (#, \$, or ‡) were statistically different from one another ($p < 0.05$ using ANOVA between groups with Tukey–Kramer significant difference post-hoc test).

to allow for conjugation to the IPN surfaces [53]. Cyclic peptides from the 7C library were synthesized as either CX₇G – denoted as (9) – or CX₇GG – denoted as (10) – where X₇ were the residues in the middle of the cysteine–cysteine loop from the sequenced library clones; these peptides were cyclized through an amide linkage between the N- and C-termini of the peptides (for structures, see Supplementary Fig. 1). The peptides bsp-RGD(15) and bsp-RGE(15), which were used as positive and negative controls in this study, have the sequences CGGNCEPRGDTYRAY and CGGNCEPRGETYRAY, respectively [12,53–55].

2.5. Adsorbed peptide surfaces

Peptides were dissolved at 100 µM in synthesis grade water, or DMSO for peptide 15-2. For adsorption to TCPS plates, solutions were sterile filtered and dried onto the plates for 3 h at room temperature in a sterile biohazard hood. NSCs were detached from laminin plates with Accutase (Innovative Cell Technologies, Inc.) and added at 30,000 cells/cm² in DMEM/F12 supplemented with 20 ng/mL FGF-2. Cells were incubated at 37 °C for 5 days with media replacement every other day. After 5 days, all media were removed, and plates were frozen at –80 °C for Cyquant (Invitrogen) cell counting, as per the manufacturer's instructions.

2.6. Interpenetrating polymer network synthesis

Interpenetrating network surfaces were synthesized as described previously [53,55]. Briefly, TCPS plates were first cleaned with 1.5 M sodium hydroxide (Sigma) dissolved in 70% ethanol (Sigma) for 1 h, followed by washing with synthesis grade water and sonication for 30 min. Before synthesis, plates were functionalized in an oxygen plasma for 5 min at 75 W power and 0.5 Torr O₂ partial pressure. The first network of the IPN was synthesized by addition of 0.1485 g/mL acrylamide (Polysciences) and 0.0015 g/mL N,N-ethylenebisacrylamide (Polysciences) as a crosslinker initiated with 0.01 g/mL [3-(4-Dimethyl-9-oxo-9H-thioxanthen-2-yloxy)-2-hydroxypropyl]trimethylammonium chloride (QTX, Sigma Aldrich) as a photoinitiator dissolved in 97% isopropyl alcohol (Sigma) and 3% synthesis grade water. After pipeting 500 µL volume into each well of a 12-well plate, plates were illuminated on a UV light table for 4.5 min. The second network was formed with 0.02 g/mL poly(ethylene glycol) monomethyl ether (MW 1000) (Polysciences) and 0.01 g/mL N,N-ethylenebisacrylamide as a crosslinker with 0.005 g/mL QTX as a photoinitiator. Acrylic acid (Polysciences) at 0.0162 mL per mL solution was also added to provide a functional site for subsequent peptide conjugation. The second network was polymerized on a UV light table for 6 min. Chains of amine-terminated PEG (MW 3400) (Laysan) at 0.150 g/mL were then grafted to the acrylic acid in the second network with 0.0025 g/mL N-hydroxysulfosuccinimide (Sulfo-NHS, Pierce) and 0.005 g/mL 1-Ethyl-3-(3-dimethylaminopropyl)carbodiimide hydrochloride (EDC, Pierce) dissolved in 0.5 M 2-(N-Morpholino)ethanesulfonic acid buffer at pH 7.0. Sulfosuccinimidyl 4-[N-maleimidomethyl]cyclohexane-1-carboxylic acid (Sulfo-SMCC, Pierce) was attached at 0.0005 g/mL in Sodium Borate Buffer at pH 7.5. Peptides were

Table 1

List of clones found with high binding avidity for neural stem cells. Clones were analyzed with flow cytometry to quantify the percentage of neural stem cells that had bacteria bound after co-incubation with the clonal bacteria population. Peptide sequences were determined via sequencing of the plasmid DNA from the bacteria. Several of the peptides exhibited homology to ECM proteins, including 7C-15, 15-52, and 7C-24 with homology to collagen, fibrinogen, and fibronectin, respectively. Also, the integrin-binding motif arginine–glycine–aspartic acid (RGD) was found in several peptides and is denoted in bold. The peptides used in further studies are highlighted in grey. The clone name indicates the library containing the clone and the data represent mean ± standard deviation.

Clone	% NSCs with Bacteria (average ± S.D.)	Peptide sequence
15–50	86.3 ± 0.8	GFVLVWSYTCCRWGK
7C-15	83.4 ± 0.8	QCCQL RGD AVCNC
15–52	82.3 ± 5.0	ESGLKVCMCKYYCMA
15–32	80.5 ± 2.0	RRELVRMTDWVVWSG
7C-1	79.4 ± 1.0	WYCFREN KYVCVM
7C-24	78.9 ± 1.7	WWCDM RGD SRCSG
Co-21	77.3 ± 5.6	MYCERDSKYWCIIH
Co-17	76.3 ± 3.0	WECAEESKFWCVF
Co-22	75.7 ± 0.8	VWCGMFGKRRCVT
15–2	73.7 ± 5.8	DHKFGLVMLNKYAYAG
7C-9	73.4 ± 1.2	KLCDFDKGYYCMR
Co-18	65.6 ± 5.9	WWCKKPEYWCIW
7C-7	65.5 ± 2.3	LECTER RGD FNCFV
Co-8	64.6 ± 5.2	WTWESAFAGRWEVGD
Co-12	54.7 ± 2.1	WVCLWHR RGDCSI
7C-20	52.4 ± 3.3	WVCIWERFKSCNE
Co-15	45.2 ± 7.2	WVCNDLIHHPCVW
7C-19	36.6 ± 3.7	WVCNKLGVYACEY

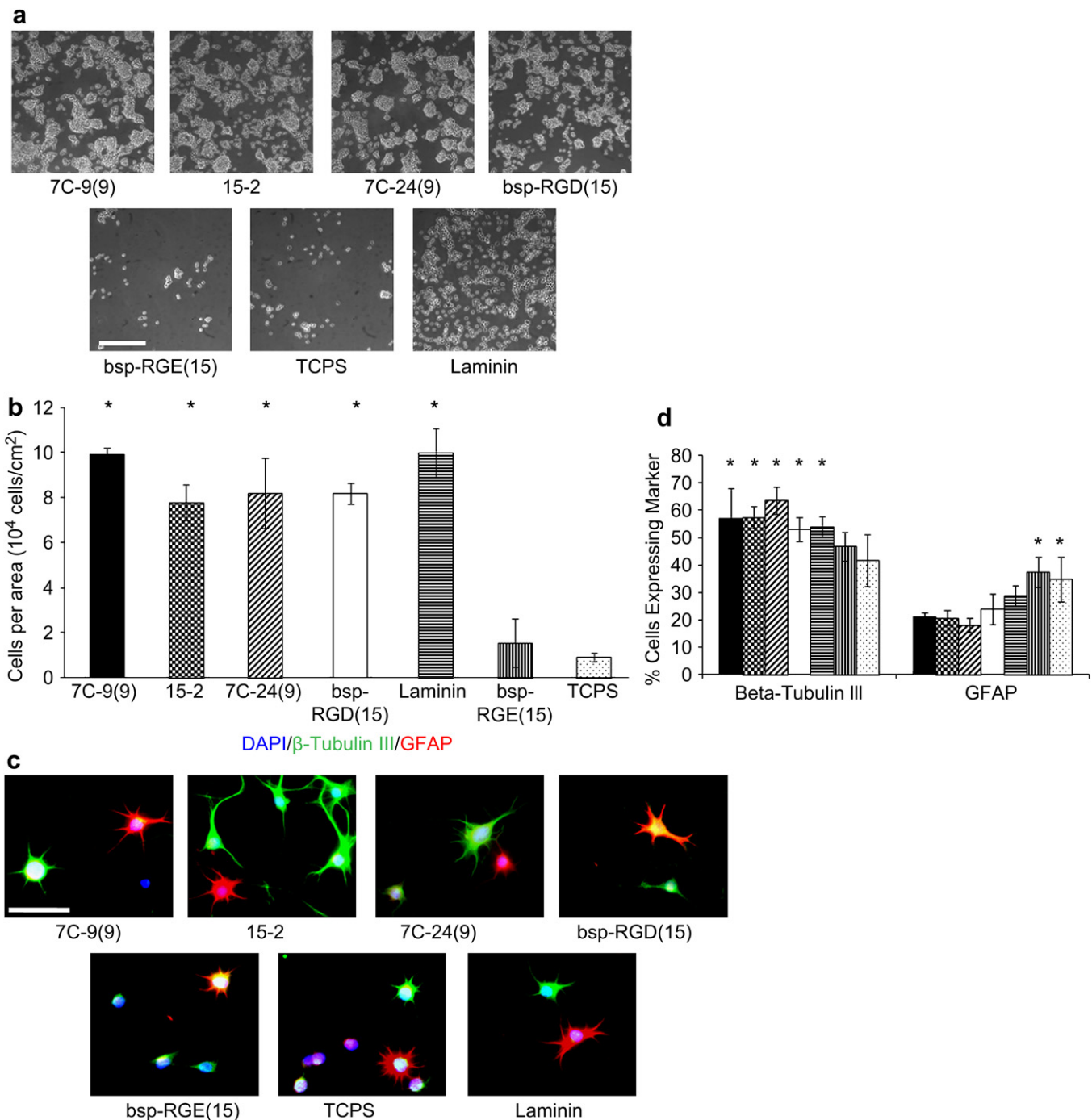


Fig. 3. Neural stem cells on peptide-adsorbed TCPS surfaces. Peptides, including (■) 7C-9(9), (▨) 7C-24(9), (▨) 15-2, (□) bsp-RGD(15), (▨) Laminin, (▨) bsp-RGE(15), and (□) TCPS alone, were dissolved at 100 μ M in synthesis-grade water or DMSO for 15–2, and then peptides were dried on TCPS. (a) Brightfield micrographs of the neural stem cells after 4 days of culture on the adsorbed surfaces exhibited similar attachment and clumping of cells on the surface on the 7C-9(9), 7C-24(9), 15-2, and bsp-RGD(15) surfaces, while the bsp-RGE(15) and TCPS surfaces had significantly fewer cells. The scale bar represents 250 μ m. (b) Quantification of the number of cells on the surface with the Cyquant cell counting assay showed similar numbers of cells on all surfaces except the bsp-RGE(15) and TCPS surfaces, which had significantly fewer cells. (c) NSCs grown under differentiating conditions were assessed for expression of GFAP (red), a cytoskeletal marker for astrocytes, and β -Tubulin III (green), a cytoskeletal marker for neurons. Nuclei were stained with DAPI (blue). All peptide surfaces had both astrocytes and neurons under differentiating conditions. All scale bars represent 100 μ m. (d) Quantification of differentiation markers, β -Tubulin III and GFAP, on peptide-adsorbed surfaces. All library-selected and bsp-RGD(15) peptide surfaces had similar percentages of neurons and astrocytes compared to laminin, while bsp-RGE(15) and TCPS surfaces had fewer neurons and more astrocytes. (Data represent mean \pm standard deviation. Library populations not in the same group (*) were statistically different from one another $p < 0.05$ using ANOVA between groups with Tukey–Kramer significant difference post-hoc test).

then attached in 0.1 M sodium phosphate buffer at pH 6.6 overnight at 4 °C via the free thiol on the terminal cysteine residue to the Sulfo-SMCC [53]. Surfaces were washed with 0.1 M sodium phosphate buffer to remove unattached peptide.

For peptide 15-2, succinimidyl 4-[N-maleimidomethyl]cyclohexane-1-carboxylate (SMCC) was first dissolved in DMSO and then diluted 1:5 in sodium borate buffer to a final concentration of 0.0005 g/mL. The peptide 15-2, which was insoluble in water, was similarly dissolved first in DMSO and then diluted 1:5 in sodium phosphate buffer. Surfaces were then washed with 1% SDS in synthesis grade water to remove unattached peptide.

2.7. Peptide density determination

For peptide surface density determination, peptides with a fluorescein isothiocyanate (FITC) tag, synthesized by American Peptide Company, were attached to IPN surfaces as described above. The fluorescent peptide sequences used were CCFDK (FITC)GYYG, CDHKPGIVMLNKK(FITC)YAYAG, and CGGNPGRGDYRAYK(FITC)GG for 7C-9(9), 15-2, and bsp-RGD(15), respectively, where the FITC residue is attached to the lysine side chain and where the 7C-9 peptide was cyclized through the N- and C-termini. After washing to remove unattached peptide, surfaces were incubated for 2 h with 1546 U/mL chymotrypsin (Calbiochem) in 10 mM Tris–HCl buffer (Invitrogen) supplemented with 1.47 mg/mL CaCl₂·2H₂O (Fisher) adjusted to pH 8.0. Fluorescence measurements were then taken on a Spectra MAX Gemini XS to calculate a final peptide concentration for each surface using an appropriate calibration curve.

2.8. Cell proliferation

For cell studies, surfaces were sterilized with 1% penicillin/streptomycin (Invitrogen) in PBS. Immediately before use, IPN surfaces were further sterilized in 70% ethanol and washed with PBS four times to remove any traces of ethanol. For proliferation studies, NSCs were detached from laminin plates and added at 30,000 cells/cm² in DMEM/F12 supplemented with 20 ng/mL FGF-2. Cells were incubated at 37 °C for 5 days with media changes every other day. After 5 days, plates were frozen at –80 °C and then assayed with CyQuant (Invitrogen).

2.9. Stem cell differentiation and immunocytochemistry

NSCs were seeded at 10,000 cells/cm² in media supplemented with 20 ng/mL FGF-2 to analyze immature neural markers, or at 18,000 cells/cm² in media supplemented with 1 μM retinoic acid (Calbiochem) and 1% fetal bovine serum (Invitrogen) for differentiating conditions. Cells were incubated at 37 °C for 5 days with media changes every other day. Cells were then stained as previously described [56,57]. Primary antibodies were incubated with cells for 48 h at 4 °C with the following dilutions: nestin antibody (BD Pharmingen) at 1:500 for proliferating conditions, and GFAP (Advanced Immunochemical, Inc.) and β-tubulin III (Sigma) at 1:1000 and 1:250 for differentiating conditions, respectively. Goat anti-mouse Alexa 488 and goat anti-rabbit Alexa 546 secondary antibodies were used at a 1:250 dilution. All images were taken on a Nikon Eclipse TE2000-E microscope.

2.10. Quantification of differentiation pictures

All cells in an image were identified and counted via DAPI staining. Cells were then manually scored as either β-tubulin III positive, GFAP positive, or indeterminate in comparison to control cells.

2.11. Statistics

All statistical analysis was carried out using ANOVA with a Tukey HSD post-hoc test. The results were considered significant at $p < 0.05$.

3. Results

3.1. Selection of peptides that bind to neural stem cells

Bacterial peptide display selections were performed on adult rat hippocampal neural stem cells (NSCs) by incubation of bacteria with NSCs and subsequent separation of the mammalian cells from unbound bacteria by centrifugation or fluorescence activated cell sorting [1,51]. Two types of peptides were used: linear X₁₅ (i.e. random 15mer peptides) and looped X₂CX₇CX₂ (i.e. 7C peptides), consisting of a random 7mer constrained by two cysteine residues that form a disulfide bond to yield a looped peptide. Both types of peptides were displayed on an engineered outer membrane protein, CPX [52]. In total, three libraries were pursued: one composed of only linear X₁₅ clones, one with only 7C cyclic clones, and a combined library containing initially equal proportions of each peptide type. To

examine the binding of various library bacterial populations to the neural stem cells after each selection step, these populations were incubated with NSCs, and the levels of bound bacteria were assessed by flow cytometry analysis of GFP, which is expressed by the *E. coli*. Representative histograms of GFP fluorescence are given for a control (empty CPX lacking a peptide insert), the unselected 7C library, and the 7C library populations after each of the three selection rounds (Fig. 2a). For instance, after three rounds of selection, the 7C library showed two clear populations, NSCs without bacteria bound at low GFP levels and NSCs with bound bacteria at high GFP levels, indicating that multiple bacteria were binding many of the NSCs. When the percentages of NSCs with bound bacteria were quantified for the various library populations with flow cytometry (Fig. 2b), we observed low binding levels for empty CPX with no peptide, unselected libraries, post round 1 libraries, and the post round 2 15mer library. However, for all other library populations, a statistical increase in binding was observed relative to bacteria expressing empty CPX. For instance, for the post round 3 libraries, there was a significant difference between the three libraries, and the 7C library had the most NSCs with bacteria bound followed by the combined library and the 15mer library.

To determine whether individual peptides from these selected pools similarly exhibited high binding levels, the binding capacities of individual bacterial clonal populations were next analyzed. After examining 60 clones, 44 were determined to have high binding, i.e. ones that have at least 30% of the NSCs with bacteria bound after co-incubation. Next, the plasmids encoding the CPX protein displaying the peptides were isolated and subjected to DNA sequencing (see Supplementary Table 1 for a complete list). Eighteen clones with a range of binding capacities were predicted to be water soluble, and thus attractive for biomaterial synthesis and modification (Table 1). In addition, several clones expressed peptides with homology to known ECM proteins based on small sequence protein basic local alignment search tool (BLAST) searches. These clones had various binding capacities ranging from 36.6% to 86.3%. Interestingly, clones 7C-15, 15-52, and 7C-24 had homology to collagen, fibrinogen, and fibronectin, respectively. In addition, four clones contained an RGD motif, well known as an important ligand motif for a subset of integrins [18,20]. These clonal data suggest that the library-based ligand selections, which were unbiased towards any ECM or integrin binding domains, yield peptides that bind to cell receptors, including integrins. Future analysis may investigate their potential receptors.

3.2. Synthetic peptides adsorbed on TCPS

Synthetic versions of three of the peptides (indicated in grey in Table 1), chosen for their high binding to NSCs and predicted water-solubility based on the ratio of charged to hydrophobic residues in the sequence, were commercially synthesized to assess their ability to support attachment and growth of NSCs. All three were tested both as adsorbed peptides on TCPS and chemically conjugated to an interpenetrating polymer network [53,58]. Two looped peptides, 7C-9 and 7C-24, were synthesized as a cyclic peptide—formed through a bond attaching the N- and C-termini—of the form CX₇G where X₇ are the amino acids from the middle of the sequenced clone (Supplementary Fig. 1). The cysteine residue was left to allow for the conjugation to the IPN, and the glycine residue was added to mimic the size of the loop in the 7C peptide clones. The residues flanking the loop from the 7C peptide clones were not incorporated synthetically, as the sterically constrained loop likely constituted the most important region of the peptide for binding. These synthetic peptides were defined as 7C-9(9) and 7C-24(9).

A linear peptide, 15-2, was synthesized with a cysteine residue on the N-terminus to allow for conjugation to various materials. bsp-

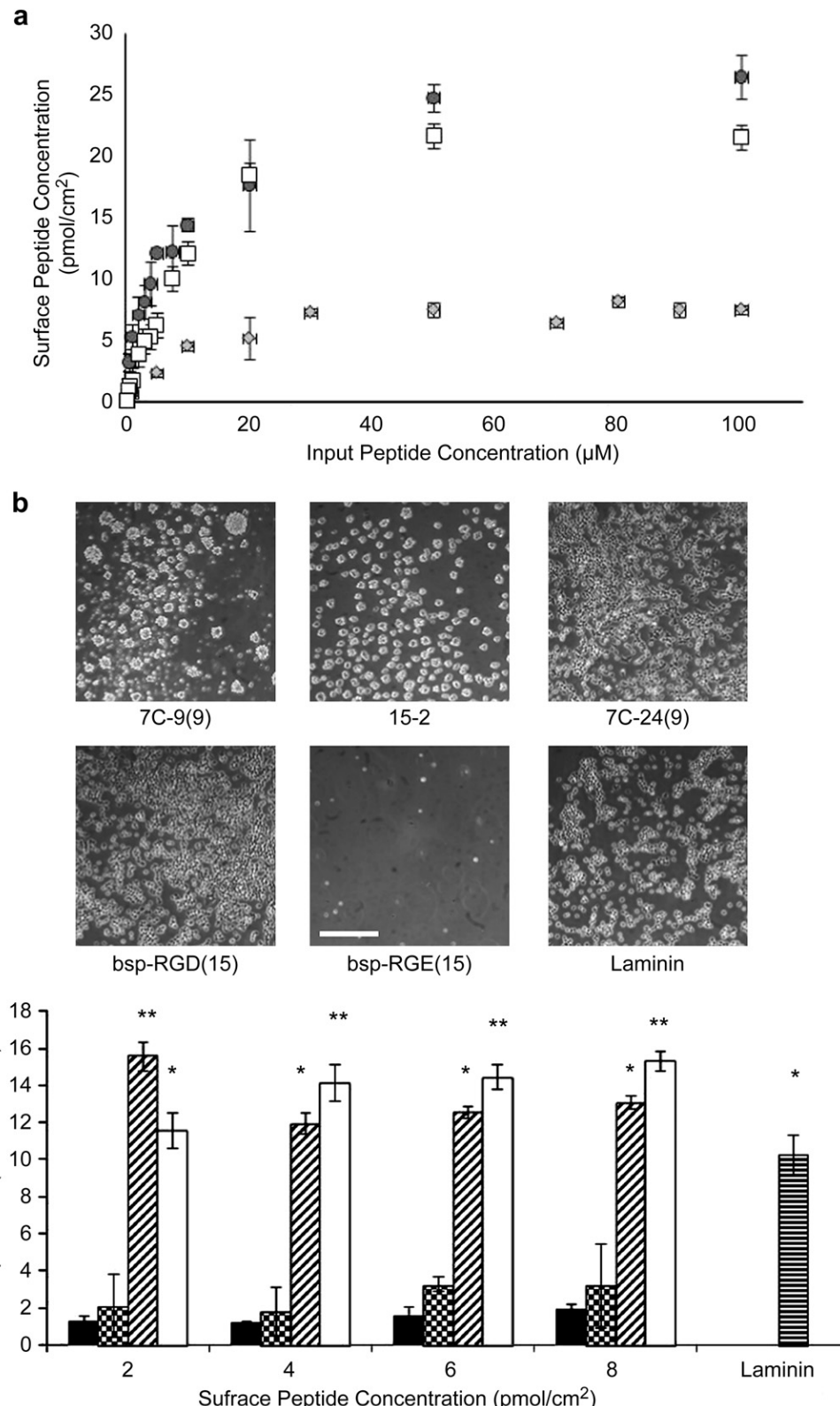


Fig. 4. Peptide grafting and cell proliferation on IPN surfaces. (a) Peptide density on interpenetrating polymer network (IPN) surfaces. Peptide densities on IPN surfaces were determined by grafting on a FITC-tagged peptide and digesting the FITC from the peptide with chymotrypsin. Fluorescent measurements then allowed for the calculation of the surface peptide concentration. Three peptides – (●) bsp-RGD(15), (□) 15-2 and (◆) 7C-9(9) – were examined. bsp-RGD(15) and 15-2 exhibited saturation at approximately 25 and 20 pmol/cm², respectively, while the looped 7C-9(9) peptide showed saturation around 8 pmol/cm². (b) Neural stem cells were cultured on interpenetrating polymer networks (IPNs) conjugated with peptides including (■) 7C-9(9), (▨) 7C-24(9), (▢) 15-2, (□) bsp-RGD(15). For comparison, neural stems were also cultured on (▨) laminin. Brightfield images after 4 days illustrated that cells on the 7C-9(9) and 15-2 surfaces either attached in clumps or remained as non-adherent neurospheres. 7C-24(9) and bsp-RGD(15) surfaces showed similar cell morphology and growth to the laminin control surface. The bsp-RGE(15)-conjugated surface showed little cell attachment. All surfaces had peptides at 8 pmol/cm², and the scale bar represents 250 μm. (c) The amount of cells on each surface after 5 days was quantified with Cyquant. 7C-24(9) and bsp-RGD(15) surfaces supported cell proliferation at or above the amount of laminin at all peptide surface concentrations. The 7C-9(9) and 15-2 surfaces had substantially fewer cells than all other surfaces, as anticipated since the cells primarily formed neurospheres rather than attaching to the surface. Results from the bsp-RGE(15) and unconjugated IPN surfaces were below the detection limit of the assay. Data represent mean ± standard deviation. Library populations not in the same group (*) or (**) were statistically different from one another ($p < 0.05$ using ANOVA between groups with Tukey–Kramer significant difference post-hoc test).

RGD(15)—a peptide previously shown to mimic NSC behavior on laminin [12]—and bsp-RGE(15)—a peptide that does not bind NSCs due to the insertion of an additional methylene in the D to E substitution that renders the peptide unable to bind integrins [12]—were used as positive and negative controls, respectively. Each of these synthetic peptides was adsorbed onto tissue culture polystyrene (TCPS), and NSCs were cultured on the resulting surfaces for 5 days (Fig. 3a). Surfaces with the three selected peptides and bsp-RGD(15) encouraged NSC attachment as clumps, while bsp-RGE(15) and TCPS with no adsorbed peptide had little cell attachment. When proliferation after 5 days was quantified (Fig. 3b), there was little cell expansion on bsp-RGE(15) and TCPS, whereas the other peptide-coated surfaces had similar levels of proliferation.

In addition to expansion, neural stem cells can undergo multipotent differentiation, a capacity tested on the peptides. Neural stem cells were cultured on the adsorbed peptides under “mixed” differentiation media conditions that encouraged differentiation into a mixture of neurons and astrocytes. After 5 days, both neurons and astrocytes were found on all surfaces as determined by β -tubulin III and glial fibrillary acid protein (GFAP) staining, respectively (Fig. 3c). When the percentages of neurons and astrocytes were quantified, all library-selected peptides were found to yield similar percentages of neurons and astrocytes to that seen on bsp-RGD(15) and laminin surfaces. In contrast, the TCPS and bsp-RGE(15) surfaces had fewer neurons and more astrocytes than laminin and the library-selected peptides (Fig. 3d). In addition, under the differentiating conditions, bsp-RGE(15) had the lowest number of cells, even in comparison to plastic surfaces with no peptide (Supplementary Fig. 2), indicating that the results observed on the peptides were entirely distinguishable from those on a peptide that does not support NSC culture. This initial study indicated that all three peptides obtained using biomimetic selections were able to encourage NSC proliferation while maintaining the NSCs in a multipotent state similar to laminin, as well as support their differentiation, making them good candidate peptides for biomaterial conjugation.

3.3. Synthetic peptides on a model biomaterial

To investigate their ability to biofunctionalize a polymer hydrogel, the activity of the peptides grafted to an interpenetrating polymer network (IPN) composed of acrylamide and poly (ethylene glycol) (PEG) networks was also determined [53,55]. To ensure that the peptide surface concentration on the IPN was consistent for all peptides, fluorescently tagged peptides were used to determine the peptide concentration at which the peptide surface concentration became saturated (Fig. 4a) [59]. The linear peptides 15-2 and bsp-RGD(15) had a saturation level of approximately 20–25 pmol/cm². In contrast, the looped peptide 7C-9(9) had a maximum surface peptide density of 8 pmol/cm², as anticipated since looped peptides cannot pack as tightly as linear peptides. For all subsequent surface experiments, all peptides were used at 8 pmol/cm² or below, thereby presenting the same surface density of ligands to the cells for all samples.

The three peptides chosen from the libraries—7C-9(9), 15-2, and 7C-24(9)—along with bsp-RGD(15) and bsp-RGE(15) were grafted onto IPN surfaces at concentrations ranging from 2 to 8 pmol/cm² (Fig. 4b and Supplementary Fig. 3). NSCs grown on IPNs with peptides 7C-9(9) or 15-2 formed neurospheres, aggregates of cells in suspension, with a few clumps of cells attached to the surface. However, the RGD-containing peptide 7C-24(9) had NSCs attached as a monolayer similar to laminin and bsp-RGD(15). IPNs conjugated with bsp-RGE(15) had very few cells attached. When proliferation after 5 days was quantified, two peptides showed very little proliferation, while the bsp-RGE(15) surfaces were below the detection limit of the assay (Fig. 4c). 7C-24(9) had proliferation at or above the

level of proliferation on laminin, and bsp-RGD(15) surfaces exhibited similar extents of cell proliferation to 7C-24(9). Thus, while two of the library-selected peptides did not support proliferation to the same extent as laminin, 7C-24(9) was able to support proliferation at or above the level of laminin, indicating the selection process successfully identified peptide sequences allowing cell adhesion and expansion.

For the looped peptides, we also investigated how the size of the loop would affect cell attachment and proliferation. Although the looped peptides expressed on the bacteria in the peptide display libraries utilized a disulfide bond to generate the loop, the synthetic peptides used in these studies were cyclized via an amide bond connecting the N- and C-termini, as the conjugation chemistry utilized a free thiol on a cysteine residue (Supplementary Fig. 1). Loop peptides of the form CX₇GG, denoted as (10) at the end of the peptide name, were also tested. Both 7C-9(10) and 7C-24(10) had similar cell attachment behavior as their smaller looped counterparts. That is, NSCs attached on 7C-9(10) surfaces formed neurospheres with some cell clumps attached, whereas cells on 7C-24(10) surfaces attached as a monolayer (Supplementary Fig. 4a). The cell proliferation after 5 days on these peptide-conjugated IPNs was compared with the smaller looped peptides (Supplementary Fig. 4b). The smaller loops supported proliferation at or above the levels of the larger loops, indicating that the smaller loops provided a better biomimetic surface.

The expression of lineage markers under proliferating and differentiating conditions was measured for NSCs cultured on the peptide-modified IPNs, with the exception of the RGE peptide that was unable to sustain cell attachment during this longer study (Fig. 5a). Under proliferating conditions with 20 ng/mL FGF-2, most NSCs on all peptide-conjugated IPNs expressed nestin, a cytoskeletal marker characteristic of an immature neural cell [60]. In addition, all peptide-conjugated IPNs supported both neuronal and glial differentiation of NSCs as indicated by expression of β -tubulin III and GFAP (glial fibrillary acidic protein), respectively, when NSCs were exposed to 1 μ m retinoic acid and 1% fetal bovine serum. When the lineage distributions were quantified under differentiating conditions (Fig. 5b), there was no appreciable difference in the numbers of astrocytes on different ligands. However, laminin surfaces had more neurons than all IPNs, and all IPNs had similar amounts of neurons. These data indicate that NSCs seeded on IPN surfaces conjugated with peptides obtained from the biomimetic ligand selections were able to self-renew under proliferative conditions and differentiate into multiple lineages under differentiating conditions. In comparison to the peptides adsorbed on TCPS, only the 7C-24(9) peptide supported the proliferation of NSCs when conjugated to the IPN, though 15-2, 7C-24(9), and 7C-9(9) each supported differentiation similar to laminin surfaces.

4. Discussion

Stem cells in general, and neural stem cells in particular, often require ECM proteins for expansion and differentiation in cell culture [4–6,61]. As the cellular signals that ECM molecules elicit are not fully or in many cases even well understood, developing a biomaterials that present isolated ligands in a controlled conformation could elucidate more about their roles in cellular signaling processes and may help identify unknown signaling domains on ECM proteins. Furthermore, the resulting fully defined systems may have utility for regenerative medicine applications. However, in part because such ECM signaling is not completely understood, designing peptides to mimic ECM proteins is difficult and often time consuming.

Fibronectin is an illustrative example of the inherent difficulty in identifying peptide ligands that recapitulate the function of the

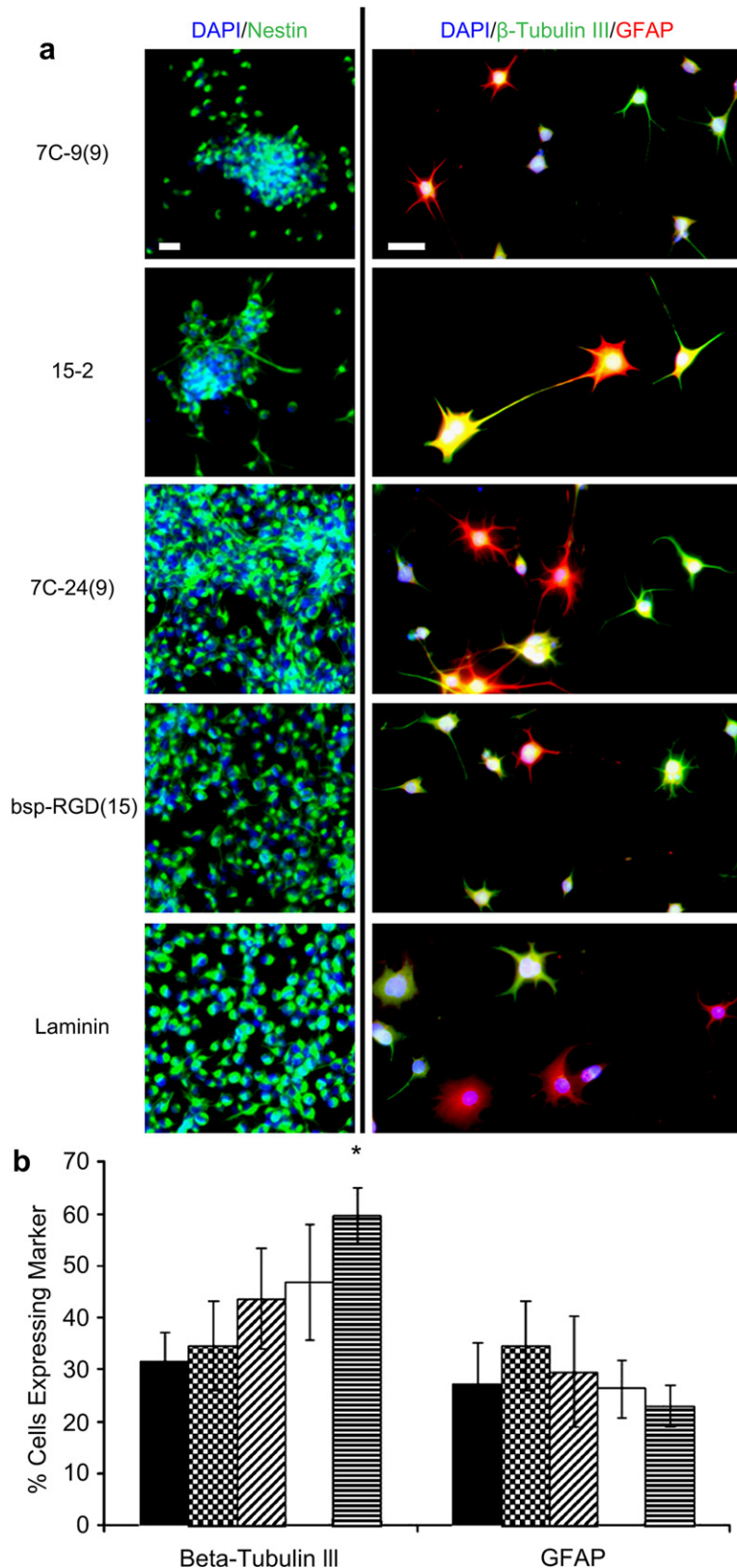


Fig. 5. Expression of lineage markers under proliferative and differentiating conditions on peptide-conjugated interpenetrating polymer networks (IPNs). Neural stem cells were cultured on the surfaces for 5 days either under proliferative conditions with 20 ng/mL basic Fibroblast Growth Factor (FGF-2) or with 1% fetal bovine serum and 1 μ M retinoic acid. (a). NSCs grown under proliferative conditions were assessed for the expression of nestin (green), a cytoskeletal marker for a neural stem cell, while NSCs grown under differentiating conditions were assessed for expression of GFAP (red), a cytoskeletal marker for astrocytes, and β -tubulin III (green), a cytoskeletal marker for neurons. All cells were stained with DAPI (blue) for the nucleus. All surfaces had most of the cells staining for nestin under proliferative conditions, and all surfaces had astrocytes and neurons under differentiating conditions. All scale bars represent 100 μ m. (b) Quantification of differentiation markers, β -tubulin III and GFAP, on (■) 7C-9(9), (▨) 15-2, (▨) 7C-24(9), (□) bsp-RGD (15), or (▨) laminin. Laminin had significantly more cells expressing β -tubulin III than any other surface, but all other surfaces had similar β -tubulin III expression. With GFAP expression there was no significant difference in expression on any surface. Data represent mean \pm standard deviation. Library populations not in the same group (*) were statistically different from one another ($p < 0.05$ using ANOVA between groups with Tukey–Kramer significant difference post-hoc test).

entire protein. While fibronectin has been known for many years to contain binding domains for integrins, only recently was the domain for α_v integrin binding found in this large ECM protein [4,37]. Additionally, even when a receptor-binding region within an ECM protein is known, very few peptides that match the sequence of the ECM motif are capable of serving as agonists for that receptor [29,30,34]. By using an unbiased library approach to find peptides with binding properties similar to ECM proteins, we have sampled a large peptide sequence space in a manner that does not require prior knowledge of the binding motifs required for cell growth and maintenance.

To find peptide candidates to replace ECM proteins, we used bacterial peptide display, which is a versatile method for peptide ligand selection for several reasons. Unlike bacteriophage libraries that require viral infections for amplification, a selected population of bacteria can be amplified by simple culturing, and the peptide valency on bacteria can be adjusted to change the selection stringency [39,49,50]. Bacterial plasmids are also easy to manipulate, allowing for easy library creation with each library containing bacteria with random peptide sequences on the bacterial surfaces. In addition, with the expression of fluorescent proteins in the library bacteria, mammalian cells with bound bacteria can be analyzed or sorted with flow cytometry for library analysis and rapid selection [48–50].

Although phage peptide display libraries have been used to find many peptides that bind to various purified integrins, most of these peptides were shown to bind to, but not to activate, these target receptors [24,40–44,62]. Cell experiments with phage display-derived peptides that bind to integrins have either focused on supporting short term cell spreading or inhibiting cell binding to ECM proteins, but longer-term assessment of the capacity of these peptides to support the culture of differentiated or stem cells have not been performed [41,44,62]. A recent study with phage display libraries found several peptide sequences that bound to human embryonic stem (hES) cells [62], but these peptides neither supported proliferation similar to Matrigel nor engaged with integrins as observed with other studies employing hES cells [14]. In addition, the peptides were displayed on self-assembled monolayer surfaces that lose stability over time and contain surface defects where cells can attach non-specifically [62–66]. Yeast peptide display libraries have been used to target the $\alpha_v\beta_3$ integrin with RGD peptides [24], but a method that is unbiased towards any particular motif is desirable, since it can allow the investigation of peptides for non-RGD binding cellular receptors.

With adult neural stem cells, our bacterial peptide display and selection approach yielded peptides with homology to small segments of ECM proteins such as collagen, fibronectin, and fibrinogen (Table 1). Furthermore, four of the selected peptides had an RGD motif, well known to bind to a subset of integrins with high affinity [20,29]. Since our biomimetic ligand selections yielded peptides with homology to ECM proteins, we hypothesize that some of the peptides that were selected may also target integrins or other important cell adhesion receptors, which future work may investigate.

In addition to finding a list of peptides that bind to NSCs, we have also explored the ability of these peptides on two different biomaterial platforms to emulate the effects of laminin, the ECM protein typically used in NSC culture. Synthetic peptides based on the sequences obtained using the selection process encouraged attachment and proliferation of NSCs to different extents in two different contexts: adsorbed on TCPS and conjugated to IPN surfaces. We used a IPN due to its modularity in controlling material properties, such as ligand density, ligand orientation, and mechanical modulus, as well as because previous studies have shown that IPNs conjugated with bsp-RGD(15) were able to mimic the effects of laminin in NSC culture [12]. In addition, the IPN has

been used to support the growth of many other cell types including osteoblasts and mesenchymal stem cells, and it has also been used as a coating on model orthopedic implants, angioplasty balloons, and stents [12,26,58,67–69].

The three synthetic peptides studied in detail were also able to support short term self-renewal and differentiation of the NSCs as indicated by studies under proliferating and differentiating conditions, respectively. All three library-selected peptides supported both self-renewal and differentiation of NSCs when adsorbed on TCPS, but only one supported both processes when conjugated on the IPN. This differential behavior observed between the same peptides when adsorbed on TCPS and conjugated on IPNs seems to indicate that the orientation of the peptide is important, as all peptides have the same orientation on the IPN, as constrained by the linkage chemistry, while the adsorbed peptide surfaces theoretically allow all possible orientations. However, in comparison to surfaces with an RGE peptide that did not support proliferation of NSCs, all of the library-selected peptides supported proliferation of NSCs and thus likely engage with cell adhesion receptors. The peptide that performed the best on the IPN contained RGD residues. This agrees with other studies that found RGD-containing peptides support NSC growth similar to laminin, indicating that the RGD-binding integrins are important for NSC engagement with matrix [12]. For example, β_1 integrins are thought to control neural stem cell self-renewal and differentiation, since they act as sensors for NSCs in the changing extracellular environment during development [3]. However, different RGD peptides likely have different specificities for the different RGD-binding integrins, such that there is value for identifying ligands. Thus, we have shown that the bacterial peptide display selection is a very powerful tool for identifying promising candidate peptides that can be conjugated to biomaterials surfaces for the growth of a desired cell type, including stem cells, indicating that these peptides may serve as receptor agonists.

5. Conclusions

Bacterial peptide display libraries are versatile and efficient tools for finding peptides for various biomaterials. The general method presented here can be applied to any desired cell type for the development of biomaterials grafted with peptides. Many peptides that bound adult neural stem cells at high levels were identified, and three of these peptides supported self-renewal and differentiation to different extents when presented either as adsorbed peptides on TCPS or conjugated to an IPN. This general platform should be helpful in discovering candidate peptides that mimic ECM signals for more complex systems such as human pluripotent stem cells.

Acknowledgements

This work was supported by funding from a graduate research fellowship from the National Science Foundation (to LL), Training Grant Number T1-00007 from the California Institute for Regenerative Medicine (to LL), and a grant from the National Institutes of Health (NIH R21DE18044).

Appendix

Figures with essential color discrimination. Figs. 1–3 & 5 in this article are difficult to interpret in black and white. The full color images can be found in the on-line version, at doi:10.1016/j.biomaterials.2010.10.032.

Appendix. Supplementary data

Supplementary data associated with this article can be found in the on-line version, at doi:10.1016/j.biomaterials.2010.10.032.

References

- [1] Palmer TD, Takahashi J, Gage FH. The adult rat hippocampus contains primordial neural stem cells. *Mol Cell Neurosci* 1997;8:389–404.
- [2] Thomson JA, Itskovitz-Eldor J, Shapiro SS, Waknitz MA, Swiergiel JJ, Marshall VS, et al. Embryonic stem cell lines derived from human blastocysts. *Science* 1998;282:1145–7.
- [3] Campos LS. Beta1 integrins and neural stem cells: making sense of the extracellular environment. *Bioessays* 2005;27:698–707.
- [4] Leiss M, Beckmann K, Giros A, Costell M, Fassler R. The role of integrin binding sites in fibronectin matrix assembly in vivo. *Curr Opin Cell Biol* 2008;20:502–7.
- [5] Tzu J, Marinkovich MP. Bridging structure with function: structural, regulatory, and developmental role of laminins. *Int J Biochem Cell Biol* 2008;40:199–214.
- [6] Yu WM, Yu H, Chen ZL. Laminins in peripheral nerve development and muscular dystrophy. *Mol Neurobiol* 2007;35:288–97.
- [7] Sastry SK, Lakonishok M, Thomas DA, Muschler J, Horwitz AF. Integrin alpha subunit ratios, cytoplasmic domains, and growth factor synergy regulate muscle proliferation and differentiation. *J Cell Biol* 1996;133:169–84.
- [8] Hakala H, Rajala K, Ojala M, Panula S, Areva S, Kellomaki M, et al. Comparison of biomaterials and extracellular matrices as a culture platform for multiple, independently derived human embryonic stem cell lines. *Tissue Eng Part A* 2009;15:1775–85.
- [9] Little L, Healy KE, Schaffer D. Engineering biomaterials for synthetic neural stem cell microenvironments. *Chem Rev* 2008;108:1787–96.
- [10] Ghosh K, Ren XD, Shu XZ, Prestwich GD, Clark RA. Fibronectin functional domains coupled to hyaluronan stimulate adult human dermal fibroblast responses critical for wound healing. *Tissue Eng* 2006;12:601–13.
- [11] Martin MJ, Muotri A, Gage F, Varki A. Human embryonic stem cells express an immunogenic nonhuman sialic acid. *Nat Med* 2005;11:228–32.
- [12] Saha K, Irwin EF, Kozhukh J, Schaffer DV, Healy KE. Biomimetic interfacial interpenetrating polymer networks control neural stem cell behavior. *J Biomed Mater Res A* 2007;81A:240–9.
- [13] Carlson JA, Garg R, Compton SR, Zeiss C, Uchio E. Poliomyelitis in SCID mice following injection of basement membrane matrix contaminated with lactate dehydrogenase-elevating virus. In: Proceedings of the 59th AALAS National Meeting; 2008. PS35.
- [14] Meng Y, Eshghi S, Li YJ, Schmidt R, Schaffer DV, Healy KE. Characterization of integrin engagement during defined human embryonic stem cell culture. *FASEB J*; 2009.
- [15] Rodin S, Domogatskaya A, Strom S, Hansson EM, Chien KR, Inzunza J, et al. Long-term self-renewal of human pluripotent stem cells on human recombinant laminin-511. *Nat Biotechnol* 2010;28:611–5.
- [16] Melkoumian Z, Weber JL, Weber DM, Fadeev AG, Zhou Y, Dolley-Sonneville P, et al. Synthetic peptide-acrylate surfaces for long-term self-renewal and cardiomyocyte differentiation of human embryonic stem cells. *Nat Biotechnol* 2010;28:606–10.
- [17] Villa-Diaz LG, Nandivada H, Ding J, Nogueira-de-Souza NC, Krebsbach PH, O’Shea KS, et al. Synthetic polymer coatings for long-term growth of human embryonic stem cells. *Nat Biotechnol* 2010;28:581–3.
- [18] Humphries JD, Byron A, Humphries MJ. Integrin ligands at a glance. *J Cell Sci* 2006;119:3901–3.
- [19] Arnaout MA, Mahalingam B, Xiong J-P. Integrin structure, allostericity, and bidirectional signaling. *Annu Rev Cell Dev Biol* 2005;21:381–410.
- [20] Hynes RO. Integrins: bidirectional, allosteric signaling machines. *Cell* 2002;110:673–87.
- [21] Petrie TA, Capadona JR, Reyes CD, Garcia AJ. Integrin specificity and enhanced cellular activities associated with surfaces presenting a recombinant fibronectin fragment compared to RGD supports. *Biomaterials* 2006;27:5459–70.
- [22] Lee MH, Adams CS, Boettiger D, Degrad WF, Shapiro IM, Composto RJ, et al. Adhesion of MC3T3-E1 cells to RGD peptides of different flanking residues: detachment strength and correlation with long-term cellular function. *J Biomed Mater Res A* 2007;81:150–60.
- [23] Drumheller PD, Hubbell JA. Polymer networks with grafted cell adhesion peptides for highly biospecific cell adhesive substrates. *Anal Biochem* 1994;222:380–8.
- [24] Silverman AP, Levin AM, Lahti JL, Cochran JR. Engineered cystine-knot peptides that bind alpha(v)beta(3) integrin with antibody-like affinities. *J Mol Biol* 2009;385:1064–75.
- [25] Rezania A, Healy KE. Integrin subunits responsible for adhesion of human osteoblast-like cells to biomimetic peptide surfaces. *J Orthop Res* 1999;17:615–23.
- [26] Bearinger JP, Castner DG, Healy KE. Biomolecular modification of p(AAm-co-EG/AA) IPNs supports osteoblast adhesion and phenotypic expression. *J Biomater Sci Polym Ed* 1998;9:629–52.
- [27] Rezania A, Thomas CH, Branger AB, Waters CM, Healy KE. The detachment strength and morphology of bone cells contacting materials modified with a peptide sequence found within bone sialoprotein. *J Biomed Mater Res* 1997;37:9–19.
- [28] Massia SP, Hubbell JA. Covalent surface immobilization of Arg-Gly-Asp- and Tyr-Ile-Gly-Ser-Arg-containing peptides to obtain well-defined cell-adhesive substrates. *Anal Biochem* 1990;187:292–301.
- [29] Ruoslahti E, Pierschbacher MD. New perspectives in cell adhesion: RGD and integrins. *Science* 1987;238:491–7.
- [30] Tashiro K, Sephel GC, Weeks B, Sasaki M, Martin GR, Kleinman HK, et al. A synthetic peptide containing the IKVAV sequence from the A chain of laminin mediates cell attachment, migration, and neurite outgrowth. *J Biol Chem* 1989;264:16174–82.
- [31] Aota S, Nomizu M, Yamada KM. The short amino acid sequence Pro-His-Ser-Arg-Asn in human fibronectin enhances cell-adhesive function. *J Biol Chem* 1994;269:24756–61.
- [32] Nomizu M, Kim WH, Yamamura K, Utani A, Song SY, Otaka A, et al. Identification of cell binding sites in the laminin alpha 1 chain carboxyl-terminal globular domain by systematic screening of synthetic peptides. *J Biol Chem* 1995;270:20583–90.
- [33] Ponce ML, Kleinman HK. Identification of redundant angiogenic sites in laminin alpha1 and gamma1 chains. *Exp Cell Res* 2003;285:189–95.
- [34] Knight CG, Morton LF, Peachey AR, Tuckwell DS, Farndale RW, Barnes MJ. The collagen-binding A-domains of integrins alpha(1)beta(1) and alpha(2)beta(1) recognize the same specific amino acid sequence, GFOGER, in native (triple-helical) collagens. *J Biol Chem* 2000;275:35–40.
- [35] Li YJ, Chung EH, Rodriguez RT, Firpo MT, Healy KE. Hydrogels as artificial matrices for human embryonic stem cell self-renewal. *J Biomed Mater Res A* 2006;79:1–5.
- [36] Reyes CD, Garcia AJ. Engineering integrin-specific surfaces with a triple-helical collagen-mimetic peptide. *J Biomed Mater Res A* 2003;65:511–23.
- [37] Takahashi S, Leiss M, Moser M, Ohashi T, Kitao T, Heckmann D, et al. The RGD motif in fibronectin is essential for development but dispensable for fibril assembly. *J Cell Biol* 2007;178:167–78.
- [38] Hartley O. The use of phage display in the study of receptors and their ligands. *J Recept Signal Transduct Res* 2002;22:373–92.
- [39] Lee S, Choi J, Xu Z. Microbial cell-surface display. *Trends Biotechnol* 2003;21:45–52.
- [40] Koivunen E, Arap W, Rajotte D, Lahdenranta J, Pasqualini R. Identification of receptor ligands with phage display peptide libraries. *J Nucl Med* 1999;40:883–8.
- [41] Koivunen E, Gay DA, Ruoslahti E. Selection of peptides binding to the alpha 5 beta 1 integrin from phage display library. *J Biol Chem* 1993;268:20205–10.
- [42] Li R, Hoess RH, Bennett JS, DeGrado WF. Use of phage display to probe the evolution of binding specificity and affinity in integrins. *Protein Eng* 2003;16:65–72.
- [43] Healy JM, Murayama O, Maeda T, Yoshino K, Sekiguchi K, Kikuchi M. Peptide ligands for integrin alpha v beta 3 selected from random phage display libraries. *Biochemistry* 1995;34:3948–55.
- [44] Murayama O, Nishida H, Sekiguchi K. Novel peptide ligands for integrin alpha 6 beta 1 selected from a phage display library. *J Biochem* 1996;120:445–51.
- [45] Schreuder MP, Brekelmans S, van den Ende H, Klis FM. Targeting of a heterologous protein to the cell wall of *Saccharomyces cerevisiae*. *Yeast* 1993;9:399–409.
- [46] Schreuder MP, Mooren AT, Toschka HY, Verrips CT, Klis FM. Immobilizing proteins on the surface of yeast cells. *Trends Biotechnol* 1996;14:115–20.
- [47] Kondo A, Ueda M. Yeast cell-surface display—applications of molecular display. *Appl Microbiol Biotechnol* 2004;64:28–40.
- [48] Bessette P, Daugherty P. Flow Cytometric screening of cDNA expression libraries for fluorescent proteins. *Biotechnol Prog* 2004;20:963–7.
- [49] Bessette P, Rice J, Daugherty P. Rapid isolation of high-affinity protein binding peptides using bacterial display. *Protein Eng Des Sel* 2004;17:731–9.
- [50] Dane K, Chan L, Rice J, Daugherty P. Isolation of cell specific peptide ligands using fluorescent bacterial display libraries. *J Immunol Methods* 2006;309:120–9.
- [51] Ray J, Peterson DA, Schinstine M, Gage FH. Proliferation, differentiation, and long-term culture of primary hippocampal neurons. *Proc Natl Acad Sci U S A* 1993;90:3602–6.
- [52] Rice J, Schohn A, Bessette P, Boulware K, Daugherty P. Bacterial display using circularly permuted outer membrane protein OmpX yields high affinity peptide ligands. *Protein Sci* 2006;15:825–36.
- [53] Bearinger JP, Castner DG, Colledge SL, Rezania A, Hubchak S, Healy KE. P (AAm-co-EG) Interpenetrating polymer networks grafted to oxide surfaces: surface characterization, protein adsorption, and cell detachment studies. *Langmuir* 1997;13:5175–83.
- [54] Harbers GM, Healy KE. The effect of ligand type and density on osteoblast adhesion, proliferation, and matrix mineralization. *J Biomed Mater Res A* 2005;75A:855–69.
- [55] Harbers GM, Gamble LJ, Irwin EF, Castner DG, Healy KE. Development and characterization of a high-throughput system for assessing cell-surface receptor-ligand engagement. *Langmuir* 2005;21:8374–84.
- [56] Hsieh J, Aimone JB, Kaspar BK, Kuwabara T, Nakashima K, Gage FH. IGF-I instructs multipotent adult neural progenitor cells to become oligodendrocytes. *J Cell Biol* 2004;164:1111–22.
- [57] Palmer TD, Markakis EA, Willhoite AR, Safar F, Gage FH. Fibroblast growth factor-2 activates a latent neurogenic program in neural stem cells from diverse regions of the adult CNS. *J Neurosci* 1999;19:8487–97.
- [58] Barber TA, Gamble LJ, Castner DG, Healy KE. In vitro characterization of peptide-modified p(AAm-co-EG/AAC) IPN-coated titanium implants. *J Orthop Res* 2006;24:1366–76.

- [59] Barber TA, Harbers GM, Park S, Gilbert M, Healy KE. Ligand density characterization of peptide-modified biomaterials. *Biomaterials* 2005;26:6897–905.
- [60] Palmer TD, Ray J, Gage FH. FGF-2-responsive neuronal progenitors reside in proliferative and quiescent regions of the adult rodent brain. *Mol Cell Neurosci* 1995;6:474–86.
- [61] Hubert T, Grimal S, Carroll P, Fichard-Carroll A. Collagens in the developing and diseased nervous system. *Cell Mol Life Sci* 2009;66:1223–38.
- [62] Derda R, Musah S, Orner BP, Klim JR, Li L, Kiessling LL. High-throughput discovery of synthetic surfaces that support proliferation of pluripotent cells. *J Am Chem Soc* 2010;132:1289–95.
- [63] Flynn N, Tran TNT, Cima MJ, Langer R. Long-term stability of self-assembled monolayers in biological media. *Langmuir* 2003;19:10909–15.
- [64] Vericat C, Vela ME, Salvarezza RC. Self-assembled monolayers of alkanethiols on Au(111): surface structures, defects and dynamics. *Phys Chem Chem Phys* 2005;7:3258–68.
- [65] Love JC, Estroff LA, Kriebel JK, Nuzzo RG, Whitesides GM. Self-assembled monolayers of thiolates on metals as a form of nanotechnology. *Chem Rev* 2005;105:1103–69.
- [66] Li Q, Chau Y. Neural differentiation directed by self-assembling peptide scaffolds presenting laminin-derived epitopes. *J Biomed Mater Res A* 2010;94:688–99.
- [67] Saha K, Keung AJ, Irwin EF, Li Y, Little L, Schaffer DV, et al. Substrate modulus directs neural stem cell behavior. *Biophys J* 2008;95:4426–38.
- [68] Barber TA, Ho JE, De Ranieri A, Virdi AS, Sumner DR, Healy KE. Peri-implant bone formation and implant integration strength of peptide-modified p(AAM-co-EG/AAC) interpenetrating polymer network-coated titanium implants. *J Biomed Mater Res A* 2007;80:306–20.
- [69] Park S, Bearinger JP, Lautenschlager EP, Castner DG, Healy KE. Surface modification of poly(ethylene terephthalate) angioplasty balloons with a hydrophilic poly(acrylamide-co-ethylene glycol) interpenetrating polymer network coating. *J Biomed Mater Res* 2000;53:568–76.